Single-process 3D-printed structures with vibration durability self-awareness

M. Palmieri[1], J. Slavič[2*], F. Cianetti[1]

[1] *University of Perugia, Department of Engineering, Via G. Duranti 93, 06125 Perugia, Italy*

[2] *University of Ljubljana, Faculty of Mechanical Engineering, Aškerčeva 6, 1000 Ljubljana, Slovenia*

Cite as:

M. Palmieri, J. Slavič, F. Cianetti, Single-process 3D-printed structures with vibration durability self-awareness, Additive Manufacturing, Volume 47, 2021, 102303, ISSN 2214-8604, https://doi.org/10.1016/j.addma.2021.102303.

Abstract

The recent advances in additive manufacturing technology allow the realization of single-process thermoplastic material extrusion (TME) 3D-printed embedded sensors, leading to the easy and inexpensive production of smart structures. While single-process TME dynamic strain sensors have already been researched, vibration durability self-awareness is more than just an additional 3D printed strain sensor and several questions need to be answered. Is the durability self-aware sensors position structure-specific? Is the fatigue life of the sensory element longer than the base structure? Does the fatigue influence the self-awareness capability? Those and several other questions are theoretically and experimentally addressed in this research. Two different fatigue identification methods are researched (i.e. the peak-response and the frequency-drop methods). It was found that the vibration durability self-aware structure printed in a single process is viable and the frequency-drop based method gives reliable fatigue estimation; the fatigue damage was correctly identified even in the case the sensory element was 3D printed in

*Corresponding author
Tel: +386-1-4771-226
Email address: janko.slavic@fs.uni-lj.si (J. Slavič)

the fatigue zone and already significantly damaged. This research opens up new capabilities for self-aware TME 3D-printed structures.

Keywords: Additive manufacturing, thermoplastic material extrusion, vibration fatigue, Smart Structures

---

1. Introduction

Smart structures can make it possible to monitor critical parameters such as the temperature, pressure or the health of components, without the need of external sensors [1]. Several advanced applications have been researched, *e.g.* in aerospace [2, 3], automotive [4] and biomedical engineering [5, 6, 7]. Additive manufacturing, especially with relatively low-cost [8] single-process TME 3D-printed smart structures [9], opens up new possibilities for sensor integration [10, 11]. It also offers various solutions for the realization of embedded sensors: a hybrid approach, where the sensing element element is inserted during the printing process [11, 12] and a multi-material TME 3D-printing [10, 9, 13].

One of the most investigated areas in recent years is the possibility of creating embedded strain sensors (exploiting the piezoresistivity effect [14, 15]) since they allow structural health monitoring [16, 17, 18]. Castro *et al.* [19] printed a piezoresistive strain sensor with a Wheatstone bridge in multiple configurations, obtaining a highly sensitive instrument. Al-Rubaiai *et al.* [20] developed a soft 3D-printed strain sensor for sensing wind. Watschke *et al.* proposed a novel design of resistive sensor for contact forces and deformation guaranteeing better response to mechanical loading if compared to capacitive sensors [21]. Maurizi et al [14] experimentally investigated the possibility of realizing dynamic strain sensors with the TME approach, showing the possibility of producing reliable dynamic sensors. More recently, research moved towards determining and optimizing sensor performance. In this context, Tan *et al.* [22] investigated the influence of the printing orientation on the electrical resistivity, Zhang *et al.* [23] studied the impact of the layer thickness, raster width, and air-gap, Watschke *et al.* [24] researched the influence of the orientation, velocity and material flow; while Hampel *et al.* [25] approached the effect of layer height, nozzle temperature and printing velocity on the electrical resistivity. Stano *et al.* [26] used a design-of-experiment approach to investigate the combination of parameters that minimized the electrical resistance and the variability of the printed sensor, discovering that the layer height and the printing orientation are the most influential parameters in terms of electrical resistance and variability. Arh *et al.*[27] introduced a method for the multiaxial identification of the dynamic piezoresistivity coefficient of TME 3D-printed structures, while Palmič *et al.* [28] investigated the optimal process parameters to achieve highly conductive printed elements for the transmission of sensor signals.

Besides the current progress in 3D-printed sensors [29], additive manufactured components frequently replace components realized with conventional processes. Several researchers are studying the structural behavior (static and dynamic) of additive manufactured components. In recent years, researchers started to focus on characterizing the fatigue behavior of TME PLA components, which is strongly influenced by several printing process parameters [30, 31, 32]. Gomez-Gras *et al.* [33] experimentally studied the influence of four parameters (layer height, infill density, nozzle diameter and velocity) on the fatigue behavior of a component made in TME PLA, verifying that the most influential parameter on fatigue life is the infill density. Afrose *et al.* [34] investigated the influence of the build orientation showing that a raster angle of 45° provides a longer fatigue life. Ezeh *et al.* [35] further confirmed the influence of the manufacturing angle on the fatigue behavior: from several experimental results obtained with non-zero mean stress, they concluded that for PLA components the mean stress can be easily taken into account by performing a fatigue assessment in terms of the maximum stress in the cycle. In 2020, Ezeh *et al.* [36] experimentally observed that the raster angle also affects the overall fatigue behavior of PLA specimens in the presence of stress concentration phenomena, although this effect was said to be negligible in these cases.

Due to the importance of the fatigue behavior of PLA additive manufactured structures and thanks to scientific progress of the last few years regarding single-process TME 3D-printed embedded sensors, the focus of this work is to experimentally investigate the possibility of realizing a single-process TME 3D-printed structure with vibration durability self-awareness. The research is based on Y-shaped specimens [37, 38], where the base material was polylactic acid (PLA) and the sensor element a piezoresistive conductive thermoplastic filament [39, 40, 14]. In order to have good confidence in the results obtainable with the printed sensor, all the outcomes were compared with those obtained from a conventional accelerometer mounted on the specimen. The parameters investigated as possible metrics for the evaluation of fatigue failure are the frequency drop [41, 42] and the peak-response variation. To be as general as possible, different geometries and positions in the structure of the additive manufactured sensor were experimentally investigated to determine whether the 3D-printed sensor can introduce a notch in the structure, resulting in a shorter fatigue life of the specimen [43].

This manuscript is organized as follows. Sec. 2 shows the process followed for the realization of the specimen and of the printed sensor. Sec. 3 introduces the experimental setup and presents the results obtained for each experimental test. Sec. 4 draws the conclusions.

2. Self aware structure preparation

In this section, the procedure used for the realization of the self-aware structure is detailed. The structure (Fig. 1) was printed with a 0.4 mm dual nozzle (Ultimaker S3) using a non-conductive material for the base structure and a conductive material for the sensory element.

2.1. The base structure

A Y-shaped specimen is frequently used for vibration fatigue research [37, 38] where the two masses attached to the free ends of the specimen are used to adjust the vibrating frequencies of the system, see Fig.1. With its adjustable natural dynamics, the Y-shaped specimen provides the possibility to achieve fatigue failure in a reasonable time and in a well-defined fatigue zone. Unlike previous studies, in this case the specimen is TME 3D-printed with a non-conductive PLA (Ultimaker pearl white) material. The main printing parameters used for the base structure are: a 0.1 mm layer height, 100 % infill density (triangular infill pattern), 0.1 mm infill layer thickness, 220 °C printing temperature, 60 °C build-plate temperature and a 70 mm/s printing speed.

The Y-specimen has several natural frequencies. The vibration fatigue was focused on excitation at the fourth natural frequency (symmetrical bending of the arms) [42] at approx. 195 Hz; the natural frequency was achieved with two masses (each of 50 grams, see Fig. 2) attached to the free ends of the Y-specimen. In order to obtain a good and repeatable fixation of the masses, it was necessary to use iron inserts, see Fig. 1. The iron insert has an external diameter of 5 mm and a M3 internal thread. To ensure a strong connection between the parts over time, the external surface of the iron insert is rough. In this way, a solid melting of the iron insert within the base structures is guaranteed. The iron inserts were inserted into a 4.9 mm hole

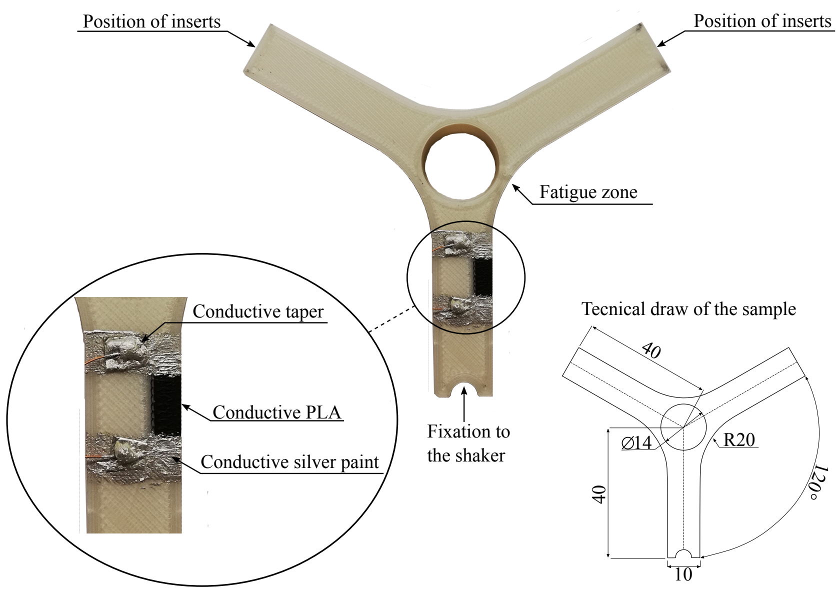

Figure 1: Preparation of the printed sensor and its electrical contacts

using a soldering tool. Between the samples, variations of approx. 1 Hz were experimentally observed.

2.2. Sensory element

A conductive PLA material (Protopasta, conductive PLA) was used for the sensory element. The sensor was printed with the specimen in a single printing process. The main printing parameters are: a 0.1 mm layer height, 100 % infill density (line infill pattern), 0.1 mm infill layer thickness, 220 °C printing temperature, 60 °C build-plate temperature and a 20 mm/s printing speed. As shown by Arh et al. [27], in order to increase the sensitivity of the sensor, the printed tracks are placed orthogonal to the measuring direction. However, different printing solution may be used anyway. To electrically connect the printed sensor to an electrical circuit, through which the voltage/resistance variation is measured, it is necessary to make electrical contacts that are mechanically strong enough to withstand the fatigue test, but at the same time light enough so as not to affect the dynamics of the system. For this purpose, the electrical contacts are realized by painting the ends of the sensor with a conductive silver paint [27, 9], see Fig. 1. The conductive silver (SCP03B produced by Electrolube) paint has a density of 1.44 g/ml, a surface resistance of 0.1 Ω/sq and a viscosity of 70 MPa s. A

1 mm thick strip of the sensor (for each end) is used for painting (Fig. 1). Once the paint is dry, it is possible to glue a conductive adhesive tape over it. Thin copper cables attached to the external measuring circuit are soldered to the conductive tape. In order to realize a better electrical contact, additional conductive paint is deposited on top of the conductive tape after the gluing process. Fig. 1 shows the realization of the sensor and of the electrical contacts.

As shown by Maurizi *et al.* [14] the dynamical load at the location of the sensor element results in changes of the resistivity. The change in resistivity was measured using the circuit shown in Fig. 2.

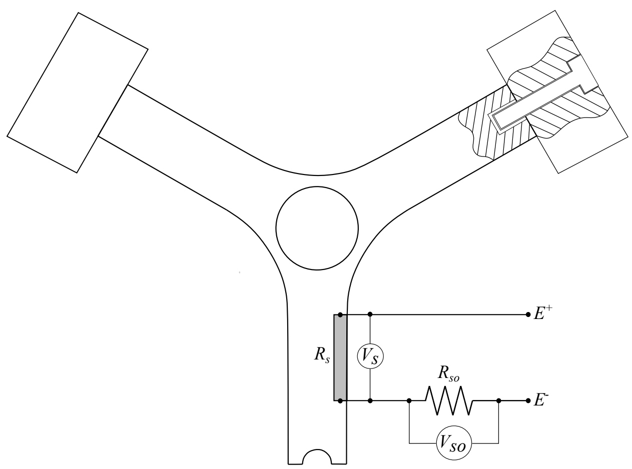

Figure 2: Schematic electrical circuit used to measure the voltage and current variation.

The realized measurement circuit allows to simultaneously measure the voltage variation V_s across the resistance of the sensors R_s and across the shunt resistor R_{so}. The shunt-resistor is used to measure the voltage drop V_{so} and to identify the current that flows along the circuit by the Ohm's law. The shunt-resistance value R_{so} is of the same order of magnitude as the printed sensor's resistance R_s [27]. Once the current I and voltage variation V_s are known, the resistance variation of the printed sensor is easily obtainable. Assuming a linear relation, it is directly related to the deformation of the structure, as with the classical strain gauges. [14]

3. Self-aware vibration durability analysis

This paragraph shows the experimental setup and the results obtained experimentally during the vibration tests carried out in order to test the ability of the printed sensor to monitor the fatigue behavior of the specimens made with additive manufacturing.

3.1. Experimental setup

To test the effectiveness of the printed sensor at monitoring the fatigue failure, the Y-shaped specimen was tested through an electrodynamic shaker in which a controlled acceleration profile has been applied at the fixation, see Fig. 3. Preliminary FE analysis allowed designed a trapezoidal Power Spectral Density (PSD), aimed to have a fatigue failure after 30 to 60 minutes, with a frequency range between 150and 200 Hz and a RMS value of 3g. The experiments were performed at room temperature; during the fatigue test, the surface temperature of the sample was monitored and no significant increase of the temperature was observed.

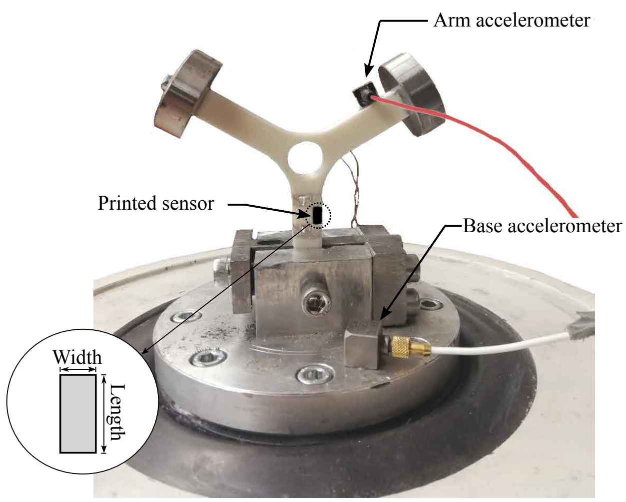

Figure 3: Experimental setup

To evaluate the sensor's ability to detect the presence of fatigue damage, an accelerometer installed on one of the arms of the specimen was used in addition to the printed sensor, Fig. 3. This allows us to compare the results of the printed sensor with those obtained with a conventional sensor used to monitor the fatigue of the components. An additional accelerometer is attached to the excitation base and is used to control the excitation profile, see Fig. 3.

In order to obtain results that are as general as possible, having the possibility to vary both the dimensions and the position of the sensor, different configurations were tested in terms of sensor width and position, simultaneously checking the sensor's performance in monitoring the fatigue failure of the structure and the influence of the sensor's position on the fatigue life. To investigate the possibility of using 3D printed sensor to monitor the fatigue life of a structural component induced by random vibration where the exact fatigue zone is not know, this manuscript researched the case where a know fatigue zone was investigated with a sensor in the fatigue zone and also out-off the fatigue zone. If the loading conditions are well know, FE analysis may be conducted in order to define the optimal location of the sensor in terms of structural strength and sensor's performances.

3.2. Sensor size and fatigue crack identification

To investigate the generality of the printed sensor to identify fatigue damage, three different sensor widths were analyzed: 1.25, 2.5, and 5 mm. The sensor length was kept constant and equal to 10 mm. To evaluate the influence of the width, the sensor was printed on the trunk of the specimen, see Fig. 3. In each test the specimen was excited with the random profile, as defined in Sec. 3.1.

To monitor the fatigue failure of the component the drop in the natural frequency was monitored; it is generally recognized that fatigue failure occurs when the natural frequency drops by 5 % with respect to its initial value [41, 42, 44]. The frequency drop is easily obtainable for lightly damped systems typical in structural dynamics application [45]. However, in case of critical damped structures a different parameter must be used to identify the fatigue behavior of the component. Fig. 4 shows a comparison of the frequency drops obtained from the embedded 3D-printed sensor and the conventional accelerometer.

As is evident from Fig. 4, the frequency drop obtained from the printed sensor is perfectly super-imposed over that obtained by the accelerometer, thus confirming the excellent effectiveness of the sensor in monitoring a possible fracture of the component. To achieve as reliable results as possible, each test has been repeated two times obtaining similar results. In each test, a fresh sample was used.

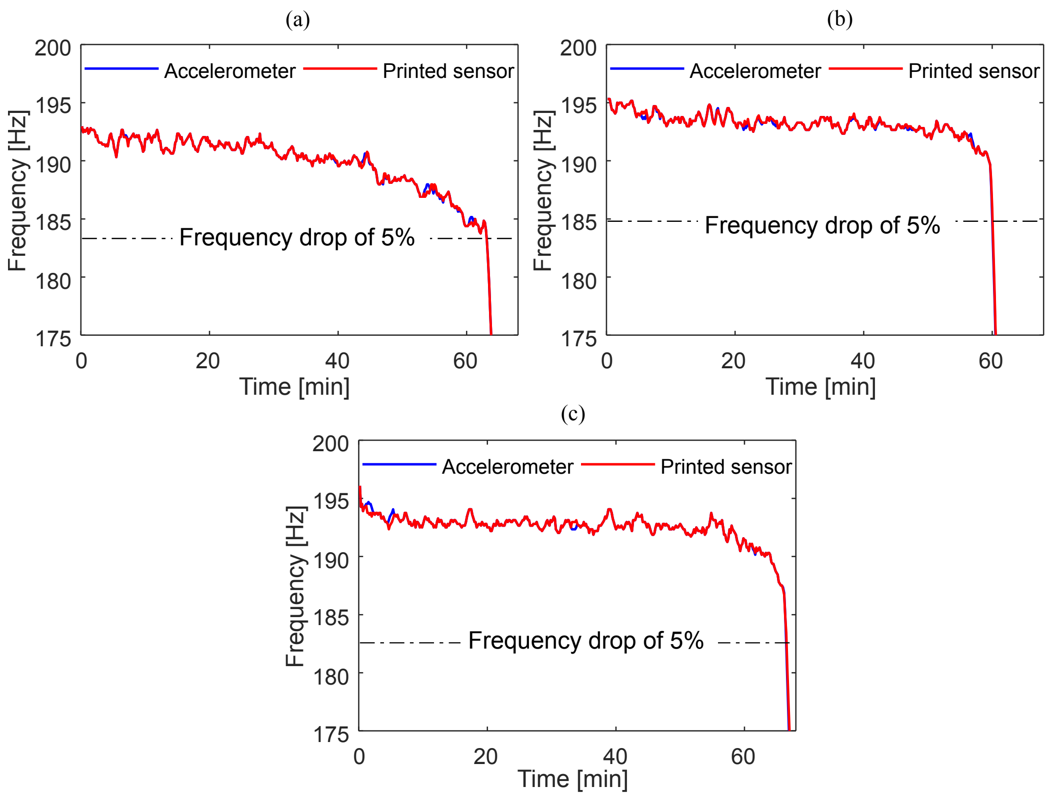

Figure 4: Comparison between frequency drop obtained by the arm accelerometer and the printed sensor. (a) Sensor width = 5 mm, (b) Sensor width = 2.5 mm, (c) Sensor width = 1.25 mm.

Besides the identified natural frequency, the response PSD peak variation could be also used for fatigue life identification. The peak-response variation acquired across the printed sensor is shown Fig.5. A comparison between the peak of the acceleration response and the voltage response for the sensor width equal to 5 mm is shown in Fig. 6. From the figures it is clear that an important drop occurs when the specimen failed due to fatigue. Indeed, comparing the results in terms of time with those shown in Fig. 4, it is clear that both approaches allow monitoring the fatigue life, at least for the researched position.

3.3. Sensor location

Beside evaluating the effect of the sensor width, another important aspect is the position of the sensor. In vibration fatigue generally, the deflec-

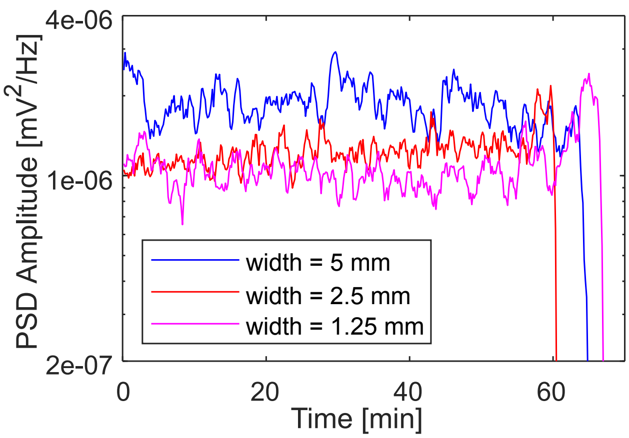

Figure 5: Comparison between peaks of the voltage PSD for the three analyzed sensor width.

tion mode excited by the excitation frequency range is not a-priori known and the location of the sensor was modified to experimentally research the importance of sensory element location for the two fatigue-damage identification methods. For this, the possibility of measuring a fatigue crack was investigated, considering five different sensor positions. Based on previous results (Sec. 3.2) only the width of 1.25 mm was used for the sensor location research. The sensor was moved up along the edge of the specimen as shown in Fig. 7.

In order to have an higher confidence of the results, the tests have been repeated two times for each positions using always a fresh specimen. The specimens were tested with the same experimental setup introduced in Sec. 3.1. As in the previous case, both the frequency drop and the peak of the PSD were observed for each specimen as possible metrics to highlight the fatigue life. Fig. 8 shows the frequency drops for the first set of specimens.

As can be seen in Fig. 8, the printed sensor is able to monitor the fatigue failure of the specimen. Indeed, visible frequency drops occur for all the specimens and the results are identical to those obtained by the accelerometer. For the second set of specimens, similar results were obtained.

As in the previous case, also in this case the possibility of using the peak of the voltage PSD measured at the ends of the printed sensor was evaluated. The trend of the peaks as a function of time is shown in Fig. 9.

From the peak of the voltage PSD at different sensor positions it is clear that while the natural frequency is correctly identified at all positions, the

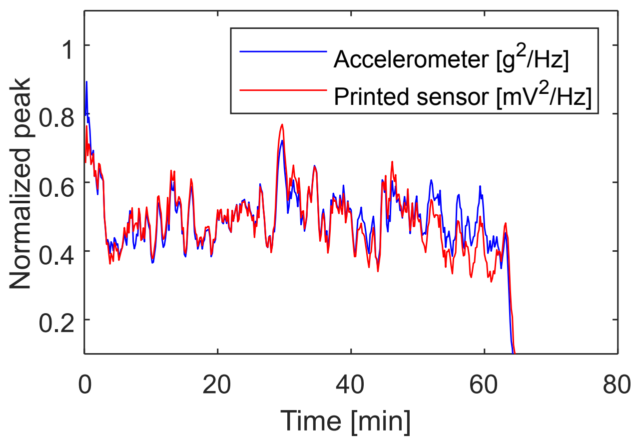

Figure 6: Comparison between the peak of the acceleration response and the voltage response (normalized respect the maximum value) for the sensor width equal to 5 mm.

Figure 7: Location of the printed sensor.

peak-response variation is highly dependent on the position. When the printed sensor enters the fatigue zone, it is reasonable to expect that the sensitivity of the sensor changes due to fatigue; however, from the results in Fig. 8 it is clear that the position of the sensor also influences the fatigue life of the whole structure. Despite the fact that the sensor is only one layer thick, it initiates the fatigue crack and the fatigue damage is significantly accelerated. As can be seen from the results shown in Fig. 8, at positions 3 and 4 of the sensor (Fig. 8 c-d) much shorter fatigue lives (approx. 50% lower) are observed than in the other cases. To highlight this aspect, Fig. 10 compares the obtained fatigue life with the sensor positions for the conducted experiment (two tests for each location). As evident, when the sensor is lo-

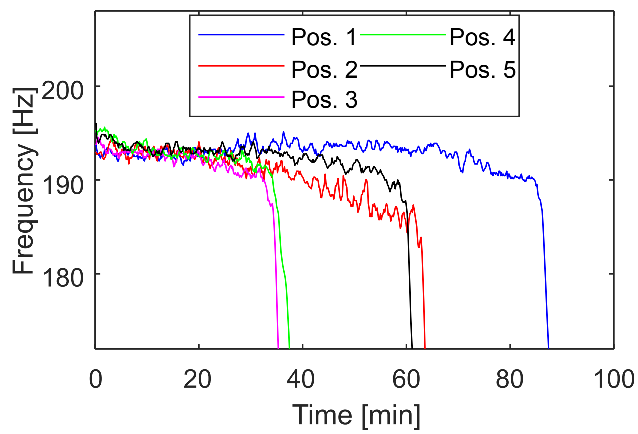

Figure 8: Frequency drop obtained by the printed sensor for each position of the sensor.

cated close to the fatigue zone, the fatigue life of the base structures is much shorter than in the other cases.

This is probably due to the fact that the fracture position is superimposed over the sensor. In fact, by monitoring the point where the fracture begins (which deviates by tenths of a millimeter between one specimen and another) with the positions 2, 3 and 4 of the sensor (see Fig. 11), it is possible to see how for positions 3 and 4 the breaking point is superimposed on the printed sensor thus inducing a premature failure of the component. The fatigue crack location for position 2 is located outside the sensor, therefore the longer fatigue life can be attributed to this [46].

Additionally, to the surface positioned sensory elements, the possibility of printing the sensor inside the structure was also researched. To this end, it was decided to print a sensor in the middle plane of the specimen, Fig. 12.

Since the previously obtained results showed the ability of the 3D printed sensor to identify a fatigue failure for each adopted position and dimension, a sensor length of 10 mm and a width equal to 5 mm was used also in the middle plane case. The external contacts are used to connect the sensor to the external measuring circuit. The specimen was excited with the same excitation profile as previously, simultaneously monitoring the accelerometer and the printed sensor. Fig. 13 shows the obtained frequency drops for the sensor printed on the middle plane of the specimen.

The failure due to fatigue is identically monitored by the accelerometer and by the printed sensor. Thus, the ability of the printed sensor to track a fatigue failure is independent of its location in the structure. Also in this

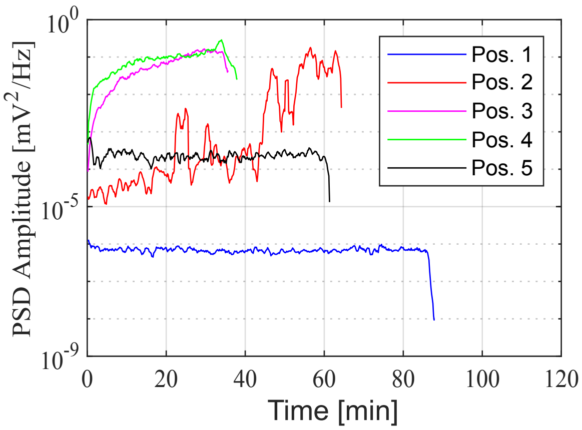

Figure 9: Comparison between the peaks of the voltage PSD for each position of the sensor.

case, from the trend of the peak of the PSD, as in shown for the previous cases, no important variations will be detected and therefore this parameter cannot be used to monitor possible fatigue failure.

3.4. Non linearity

In prior sections the linearity of the tested structure was assumed; not to make the mistake and excite the structure in a non-linear region, here the linearity assumption will be experimentally checked. To this end, the 1.25 mm width sensor in position 1 shown in Fig. 7 was tested by exciting it with a sine wave with a constant frequency of 150 Hz and linearly increasing the amplitude from 0.1 g to 10 g in 10 s. A sine wave frequency of 150 Hz was chosen in order to not excite the natural frequency of the specimen (which is around 195 Hz), but at the same time not to be close to the natural frequency (due to the uncertainty associated with in-natural frequency excitation). The maximum value of the excitation amplitude 10 g was considered in order to have a test without fatigue failure for, at least, 10 seconds. During these tests, none of the specimens failed.

The non-linearity test was repeated three times, always with a fresh specimen. Fig. 14 shows the responses obtained from both the accelerometer and the printed sensor. The 3D-printed sensor sensitivity is obviously not constant between different prints, but is in the researched range close to linear, see Fig. 14.

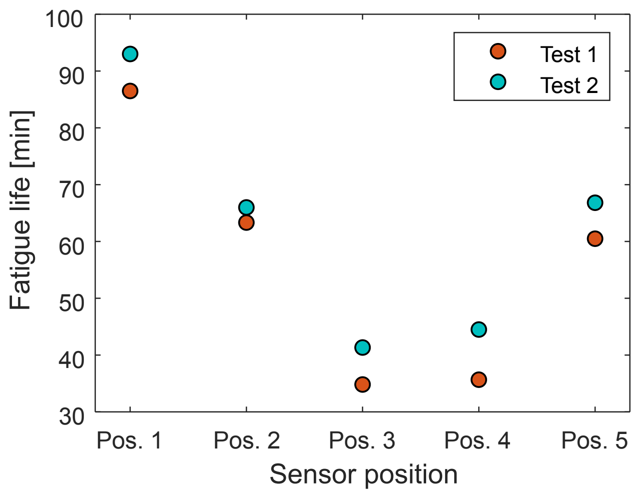

Figure 10: Fatigue life of the structure vs sensor position

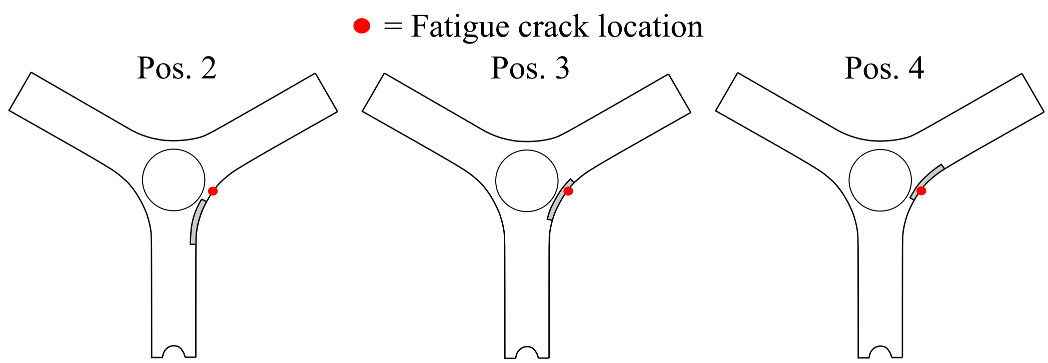

Figure 11: Location of the fatigue crack vs position of the sensor

To further evaluate the linearity of the sensors, the linear regression (of the form $y = k\,x$, where x is the acceleration excitation amplitude and y is the response acceleration amplitude or the response voltage amplitude, respectively) has been performed to determine the parameter k. For the accelerometer, the coefficients k are 1.180, 1.315 and 1.440 for test 1, test 2 and test 3, respectively; while for the 3D-printed sensor the coefficients k were $9.485 \cdot 10^{-5}\,\mathrm{V\,s^2/m}$, $8.123 \cdot 10^{-5}\,\mathrm{V\,s^2/m}$ and $7.222 \cdot 10^{-5}\,\mathrm{V\,s^2/m}$ for test 1, test 2 and test 3, respectively. To better define the linearity, the R-squared values (R^2) was computed and it is shown in Fig. 14. For the accelerometer, the R^2 is equal to 1.0000, 0.9999 and 1.0000 for each test respectively, while for the 3D-printed sensor the computed R^2 corresponds to 0.9991, 0.9994 and

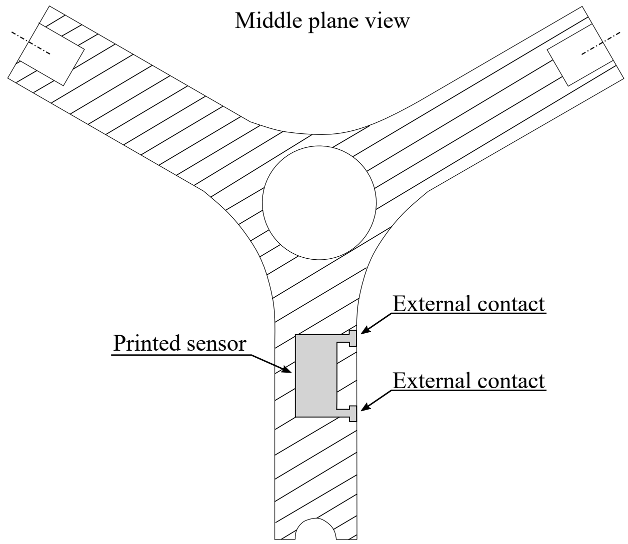

Figure 12: Sensor printed in the middle plane of the structure (at 5mm of height).

0.9999 confirming the linear behavior of both the accelerometer and of the 3D-printed strain sensor.

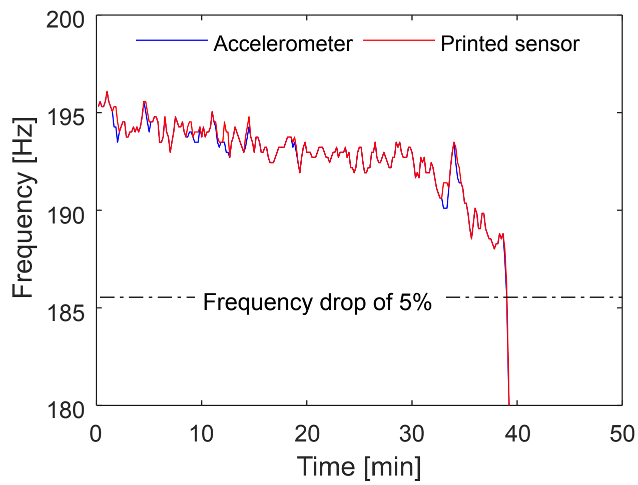

Figure 13: Comparison between frequency drop obtained by accelerometer and middle-plane printed sensor

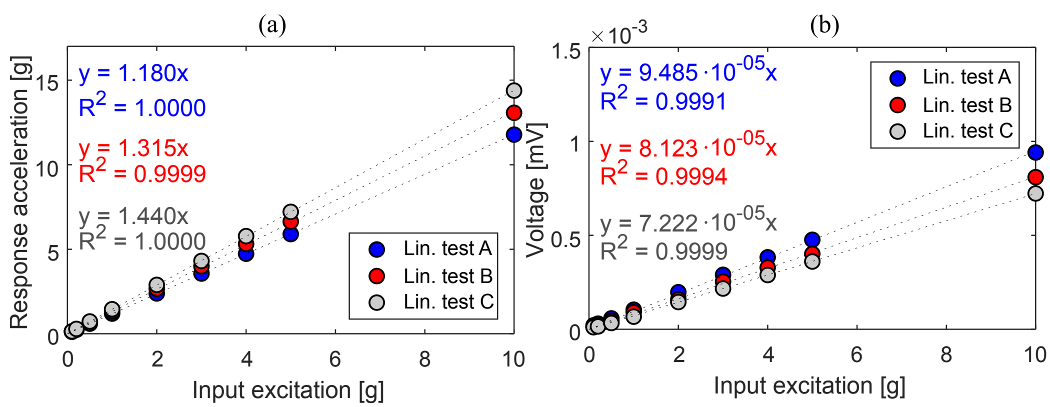

Figure 14: Behavior of the printed sensor for different amplitude excitation values. (a) Accelerometer response; (b) Printed sensor response

4. Conclusion

The possibility of using a 3D-printed embedded strain sensor of simple geometry to monitor the fatigue behavior and the fatigue life of a additive manufactured mechanical component subjected to a random excitation was researched. The position of the sensor element in the base structure, the influence of the sensor dimension and the fatigue behavior of the sensor element were investigated. Two different methods (the frequency drop and the variation of the peak-response) were investigated for fatigue damage monitoring.

The Y-shaped specimen was excited with a controlled base acceleration and the results obtained from the in-situ 3D printed strain sensor were compared to those of a classical accelerometer. The obtained results show that with the researched sensor widths and the researched positions (in the middle plane of the structure, far from or close to the fatigue zone), the sensor is always able to provide the information for fatigue damage identification. The most accurate fatigue damage identification method is the frequency-drop which is always able to correctly identify fatigue damage, the response-peak variation method is instead not always reliable.

The changes of the sensor's position allowed noticing that the sensor location has a great influence on the fatigue strength of the base structure. Indeed, the closer the sensor is to the fatigue zone, the shorter is the fatigue life of the specimen. This is due to the discontinuity of the material introduced by the sensor that causes the initiation of a fracture.

The results obtained in this research confirmed the potential of durability self-aware TME 3D-printed structures.

Acknowledgement

The authors acknowledge the partial financial support from the Slovenian Research Agency (research projects N2-0144 and J2-1730).

References

[1] Y. Xu, X. Wu, X. Guo, B. Kong, M. Zhang, X. Qian, S. Mi, W. Sun, The boom in 3d-printed sensor technology, Sensors 17 (2017).

[2] H. Boukabache, C. Escriba, J.-Y. Fourniols, Toward smart aerospace structures: Design of a piezoelectric sensor and its analog interface for flaw detection, Sensors 14 (2014) 20543–20561.

[3] A. Basheer, Advances in the smart materials applications in the aerospace industries, Aircraft Engineering and Aerospace Technology 92 (2020) 1027–1035.

[4] M. O. F. Emon, J.-W. Choi, Flexible piezoresistive sensors embedded in 3d printed tires, Sensors 17 (2017).

[5] T. Han, S. Kundu, A. Nag, Y. Xu, 3d printed sensors for biomedical applications: A review, Sensors 19 (2019).

[6] M. Sharafeldin, A. Jones, J. F. Rusling, 3d-printed biosensor arrays for medical diagnostics, Micromachines 9 (2018).

[7] I. Rojek, D. Mikołajewski, E. Dostatni, M. Macko, Ai-optimized technological aspects of the material used in 3d printing processes for selected medical applications, Materials 13 (2020).

[8] S. Leigh, R. Bradley, C. Purssell, D. Billson, D. Hutchins, A simple, low-cost conductive composite material for 3d printing of electronic sensors, PLoS ONE 7(11) (2012) 156–163.

[9] M. Arh, J. Slavič, M. Boltežar, Design principles for a single-process 3d-printed accelerometer – theory and experiment, Mechanical Systems and Signal Processing 152 (2021).

[10] M. O. F. Emon, F. Alkadi, D. G. Philip, D.-H. Kim, K.-C. Lee, J.-W. Choi, Multi-material 3d printing of a soft pressure sensor, Additive Manufacturing 28 (2019) 629–638.

[11] M. S. Hossain, J. A. Gonzalez, R. M. Hernandez, M. A. I. Shuvo, J. Mireles, A. Choudhuri, Y. Lin, R. B. Wicker, Fabrication of smart parts using powder bed fusion additive manufacturing technology, Additive Manufacturing 10 (2016) 58–66.

[12] C. Kim, C. Sullivan, A. Hillstrom, R. Wicker, Intermittent embedding of wire into 3d prints for wireless power transfer, International Journal of Precision Engineering and Manufacturing 22 (2021) 919–931.

[13] A. Bellacicca, T. Santaniello, P. Milani, Embedding electronics in 3d printed structures by combining fused filament fabrication and supersonic cluster beam deposition, Additive Manufacturing 24 (2018) 60–66.

[14] M. Maurizi, J. Slavič, F. Cianetti, M. Jerman, J. Valentičič, A. Lebar, M. Boltežar, Dynamic measurements using FDM 3D-Printed embedded strain sensors, Sensors 19 (2019).

[15] D. Chung, A critical review of piezoresistivity and its application in electrical-resistance-based strain sensing, Journal of Materials Science volume 55 (2020) 15367–15396.

[16] N. Munasinghe, M. Woods, L. Miles, G. Paul, 3-d printed strain sensor for structural health monitoring, in: 2019 IEEE International Conference on Cybernetics and Intelligent Systems (CIS) and IEEE Conference on Robotics, Automation and Mechatronics (RAM), pp. 275–280.

[17] D. Zymelka, K. Togashi, T. Kobayashi, Carbon-based printed strain sensor array for remote and automated structural health monitoring, Smart Materials and Structures 29 (2020) 105022.

[18] M. Le, F. Ganet, D. Audigier, J. Capsal, P. Cottinet, Printing of microstructure strain sensor for structural health monitoring, Appl. Phys. A 123 (2017).

[19] H. Castro, V. Correia, N. Pereira, P. Costab, J. Oliveiraa, S. Lanceros-Méndez, Printed wheatstone bridge with embedded polymer based piezoresistive sensors for strain sensing applications, Additive Manufacturing 20 (2018) 119–125.

[20] M. Al-Rubaiai, R. Tsuruta, U. Gandhi, C. Wang, X. Tan., A 3d-printed stretchable strain sensor for wind sensing, Smart Mater. Struct. 28 (2019) 084001.

[21] H. Watschke, M. Goutier, J. Heubach, T. Vietor, K. Leichsenring, M. Böl, Novel resistive sensor design utilizing the geometric freedom of additive manufacturing, Applied Sciences 11 (2021).

[22] J. Tan, H. Low, Embedded electrical tracks in 3d printed objects by fused filament fabrication of highly conductive composites, Additive Manufacturing 23 (2018) 294–302.

[23] J. Zhang, N. Wang, L. Yuan, F. Chen, K. Wu, Discrimination of winter wheat disease and insect stresses using continuous wavelet features extracted from foliar spectral measurements, Biosystems Engineering 162 (2017) 20–29.

[24] H. Watschke, K. Hilbig, T. Vietor, Design and characterization of electrically conductive structures additively manufactured by material extrusion, Applied Sciences 9 (2019).

[25] B. Hampel, S. Monshausen, M. Schilling, Properties and applications of electrically conductive thermoplastics for additive manufacturing of sensors, Technisches Messen 84 (2017) 593–599.

[26] G. Stano, A. Di Nisio, A. Lanzolla, M. Ragolia, G. Percoco, Fused filament fabrication of commercial conductive filaments: experimental study on the process parameters aimed at the minimization, repeatability and thermal characterization of electrical resistance, The International Journal of Advanced Manufacturing Technology 11 (2020) 2971–2986.

[27] M. Arh, J. Slavič, M. Boltežar, Experimental identification of the dynamic piezoresistivity of fused-filament-fabricated structures, Additive Manufacturing 36 (2020) 101493.

[28] T. Barši Palmić, J. Slavič, M. Boltežar, Process parameters for fff 3d-printed conductors for applications in sensors, Sensors 20 (2020).

[29] M. R. Khosravani, T. Reinicke, 3d-printed sensors: Current progress and future challenges, Sensors and Actuators A: Physical 305 (2020) 111916.

[30] R. Jerez-Mesa, J. Travieso-Rodriguez, J. Llumà-Fuentes, G. Gomez-Gras, D. Puig, Fatigue lifespan study of pla parts obtained by additive manufacturing, Procedia Manufacturing 13 (2017) 872–879.

[31] L. Safai, J. S. Cuellar, G. Smit, A. A. Zadpoor, A review of the fatigue behavior of 3d printed polymers, Additive Manufacturing 28 (2019) 87–97.

[32] S. Valvez, P. N. B. Reis, L. Susmel, F. Berto, Fused filament fabrication-4d-printed shape memory polymers: A review, Polymers 13 (2021).

[33] G. Gomez-Gras, R. Jerez-Mesa, J. A. Travieso-Rodriguez, J. Lluma-Fuentes, Fatigue performance of fused filament fabrication pla specimens, Materials & Design 140 (2018) 278–285.

[34] M. Afrose, S. H. Masood, P. Iovenitti, M. Nikzad, I. Sbarski, Effects of part build orientations on fatigue behaviour of fdm-processed pla material, Progress in Additive Manufacturing 1 (2016) 21–28.

[35] O. Ezeh, L. Susmel, Fatigue strength of additively manufactured polylactide (pla): effect of raster angle and non-zero mean stresses, International Journal of Fatigue 126 (2019) 319–326.

[36] O. Ezeh, L. Susmel, On the notch fatigue strength of additively manufactured polylactide (pla), International Journal of Fatigue 136 (2020) 105583.

[37] M. Česnik, J. Slavič, Vibrational fatigue and structural dynamics for harmonic and random loads, Strojniski Vestnik/Journal of Mechanical Engineering 60 (2014) 339–348.

[38] M. Palmieri, M. Česnik, J. Slavič, F. Cianetti, M. Boltežar, Non-gaussianity and non-stationarity in vibration fatigue, International Journal of Fatigue 97 (2017) 9–19.

[39] P. F. Flowers, C. Reyes, S. Ye, M. J. Kim, B. J. Wiley, 3d printing electronic components and circuits with conductive thermoplastic filament, Additive Manufacturing 18 (2017) 156–163.

[40] A. Fiorillo, C. Critello, S. Pullano, Theory, technology and applications of piezoresistive sensors: A review, Sensors and Actuators A: Physical 281 (2018) 156–175.

[41] J. T. Kim, Y. S. Ryu, H. M. Cho, N. Stubbs, Damage identification in beam-type structures: frequency-based method vs mode-shape-based method, Engineering Structures 25 (2003) 57–67.

[42] M. Mršnik, J. Slavič, M. Boltežar, Multiaxial vibration fatigue—a theoretical and experimental comparison, Mechanical Systems and Signal Processing 76-77 (2016) 409–423.

[43] R. Smith, K. Miller, Fatigue cracks at notches, International Journal of Mechanical Sciences 19 (1977) 11–22.

[44] G. Morettini, C. Braccesi, F. Cianetti, S. Razavi, Design and implementation of new experimental multiaxial random fatigue tests on astm-a105 circular specimens, International Journal of Fatigue 142 (2021) 105983.

[45] N. Maia, S. Montal$\tilde{v}$ao, Theoretical and Experimental Modal Analysis, England: Research Studies Press, Taunton (UK), sixth edition, 1997.

[46] J. Collins, Failure of materials in mechanical design: analysis, prediction, prevention, John Wiley & Sons, Hoboken, first edition, 1993.